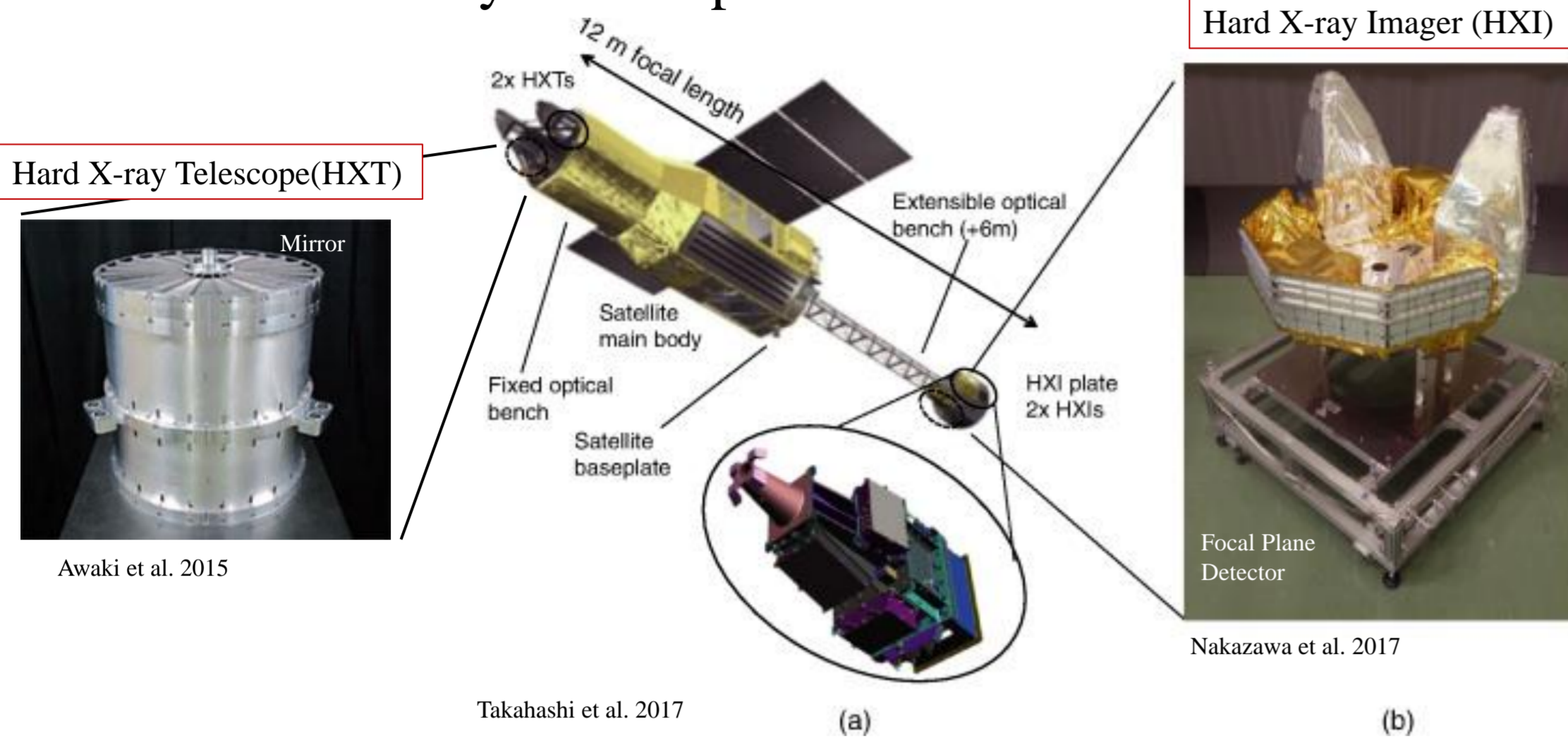


Image deconvolution of the Crab Nebula observed by Hitomi/HXT

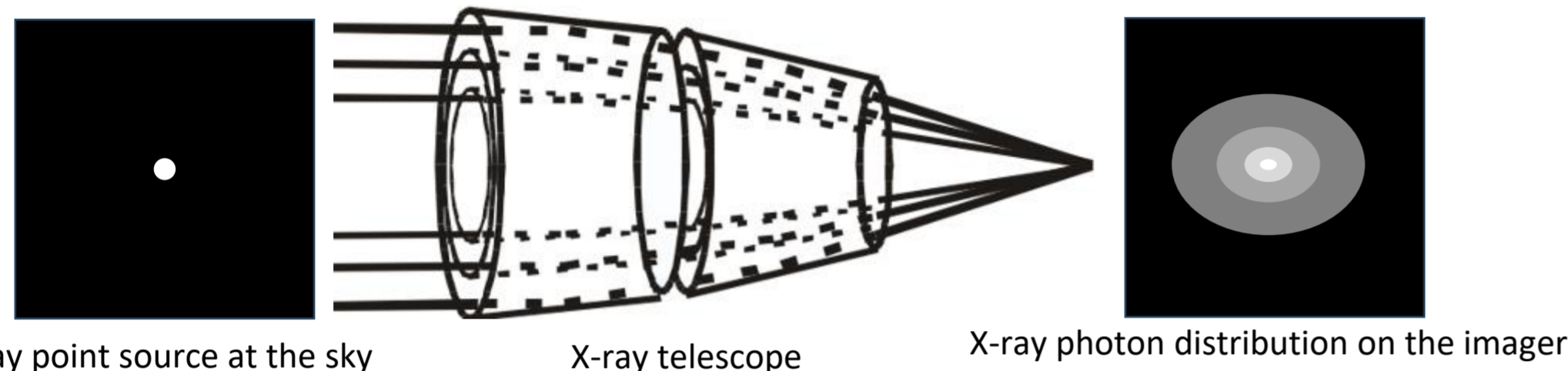
Mikio Morii (JAXA, DATUM STUDIO Co. Ltd.), Yoshitomo Maeda (JAXA), Hisamitsu Awaki (Ehime Univ.), Kouichi Hagino (Univ. of Tokyo), Manabu Ishida (JAXA) and Koji Mori (Univ. of Miyazaki)

We develop a new deconvolution method to recover the Crab Nebula image taken by the Hitomi/HXT. To suppress the artifact due to the bright Crab pulsar located at the center of the Crab Nebula, we extend the Richardson-Lucy method. Here, we introduce two components corresponding to the nebula and pulsar with regularization for smoothness and flux, respectively, and we perform simultaneous deconvolution of multi-pulse-phase images. At 3.6-15 keV band, we successfully recover the torus and jets, as seen in the Chandra X-ray image. Above 15 keV, we confirm the NuSTAR's findings that the nebula size decreases in higher energy bands.

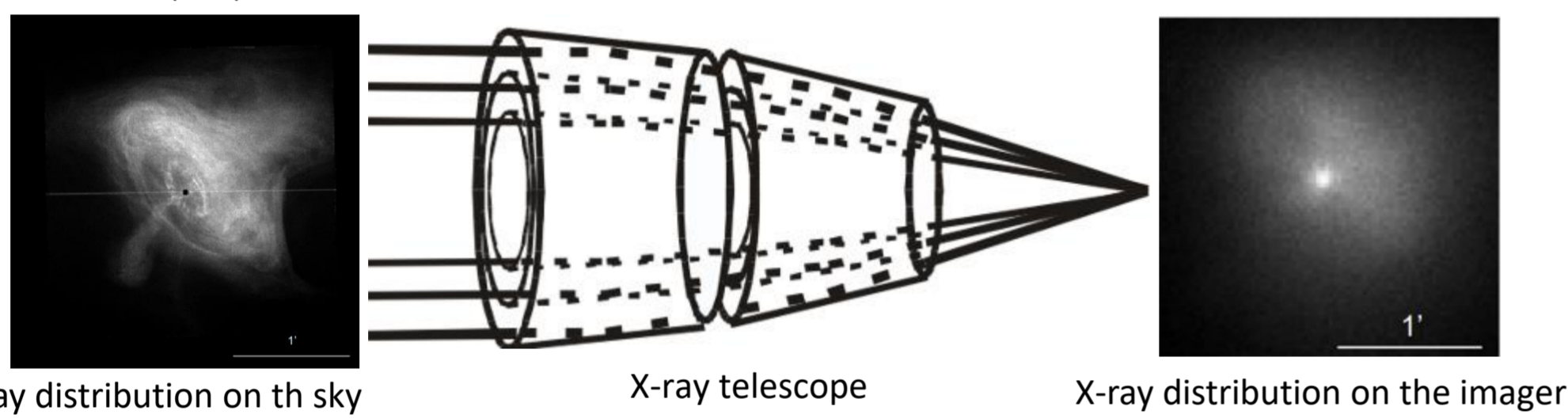
Hitomi / Hard X-ray Telescope



Observed image is a super-position of the Point Spread Function

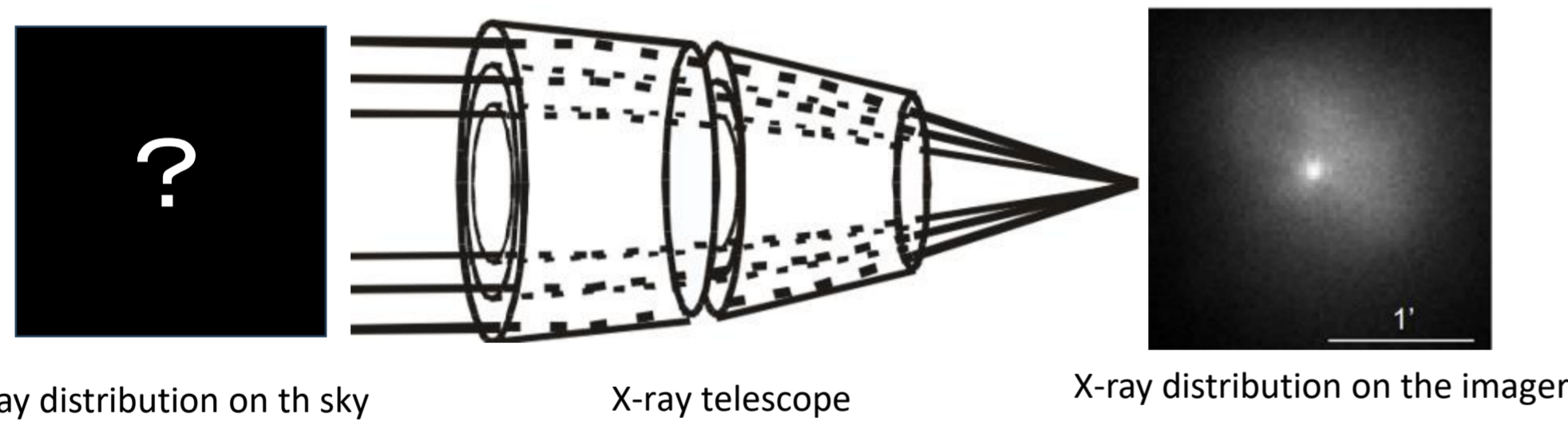


X-rays from a point source on the sky pass through an X-ray telescope and detected by an imager at the focal plane. The X-ray distribution is spread out on the imager. The X-ray distribution on the imager is called the Point Spread Function (PSF).



Since X-ray distribution on the sky is the superposition of X-ray point sources, X-ray distribution on the imager is the superposition of PSF.

Inference of X-ray distribution on the sky (Inverse Problem)



- When the average number of X-ray photons detected on a camera pixel is N , the number of X-ray photons at the pixel (Y) follow Poisson probability distribution with mean of N .
- The number of X-ray photons at each camera pixel (Y) is a random variable and mutually independent.
- X-ray distribution at the sky consists of two components: pulsar component (point source) and nebula component.
- Pulsar component has periodical time variation, while nebula component has no time variation.
- Nebula component has a smooth distribution.

We infer the most likely X-ray distribution on the sky with satisfying these conditions. Image Deconvolution.

Extension of Richardson-Lucy method (Bayesian Inference)

- Two component model: pulsar (point source with fixed position) + Nebula
- Assume smoothness for the nebula component.
- Pulsar component is far brighter than nebula, then nebula shape around pulsar deforms.
- To reduce the artifact, we introduce regularization for pulsar flux.
- Pulsar component changes along with pulse phases, while nebula component is constant.

Combined multi pulse phase image deconvolution

- Sky image is divided into pixels (index: $u = 1, \dots, M$). Index of HXI pixels: $v=1, \dots, V$.
- Camera ID ($c = 1, 2$ for HXI-1, HXI-2).
- Response matrix of HXT(including HXI) is $t_{c,v,u}$ (Point Spread Function).
- We use HXI images of 10 pulse phases ($Y_{c,p,v}$) ($p = 1, 2, \dots, 10$ phases).
- Position of Crab pulsar is known (fix). Flux of Crab pulsar is unknown (free).
- Flux of Crab pulsar in phase p is f_p . Image of Crab Nebula is unknown (free): I_u .
- Image of Crab pulsar is $I_{0,u}$ (1: for the pulsar position, 0: for the others).
- Image of particle background is $b_{c,v}$.
- Width of pulse phase of p : $(\Delta\phi)_p (= 0.1)$.
- HXIs have dead time. Fraction of active time of HXI is Live Time Fraction $(F_{lt})_{c,p} \sim 0.75$, they depend on pulse phase.
- The number of events in pixel v of counter c in an exposure of pulse phase p is $Y_{c,p,v}$. It follows a Poisson distribution:

$$Y_{c,p,v} \sim \text{Poisson} \left\{ \left[\sum_u t_{c,v,u} (I_u + f_p I_{0,u}) + b_{c,v} \right] (\Delta\phi)_p (F_{lt})_{c,p} \right\}$$

Likelihood

$$p(Y|I, f) = \prod_{p=1}^{n_p} \prod_{v=1}^V \text{Poisson} \left\{ Y_{p,v}; \left[\sum_{u=1}^M t_{v,u} (I_u + f_p I_{0,u}) + b_v \right] (\Delta\phi)_p (F_{lt})_p \right\}$$

Smooth regularization (Nebula component)

Prior probability distribution for I_u is

$$p_{\text{smooth}}(I) = Z_I \exp[-\mu V(I)] \quad (10)$$

Here,

$$V(I) = \sum_{(r,s) \in \mathcal{N}} (I_r - I_s)^2 \quad (11)$$

$$= \sum_{i=1}^{m-1} \sum_{j=1}^{n-1} [(I_{i,j} - I_{i+1,j})^2 + (I_{i,j} - I_{i,j+1})^2] \quad (12)$$

$$+ \sum_{i=1}^{m-1} (I_{i,n} - I_{i+1,n})^2 + \sum_{j=1}^{n-1} (I_{m,j} - I_{m,j+1})^2 \quad (13)$$

Z_I is a normalization factor. $\mu > 0$ is a hyper-parameter.

Pulse profile regularization (Pulsar component)

Prior probability distribution for f_p is

$$p_{\text{flux}}(f) = Z_f \exp[-\gamma D(f)] \quad (14)$$

Here,

$$D(f) = \sum_p (f_p - f_{0,p})^2 \quad (15)$$

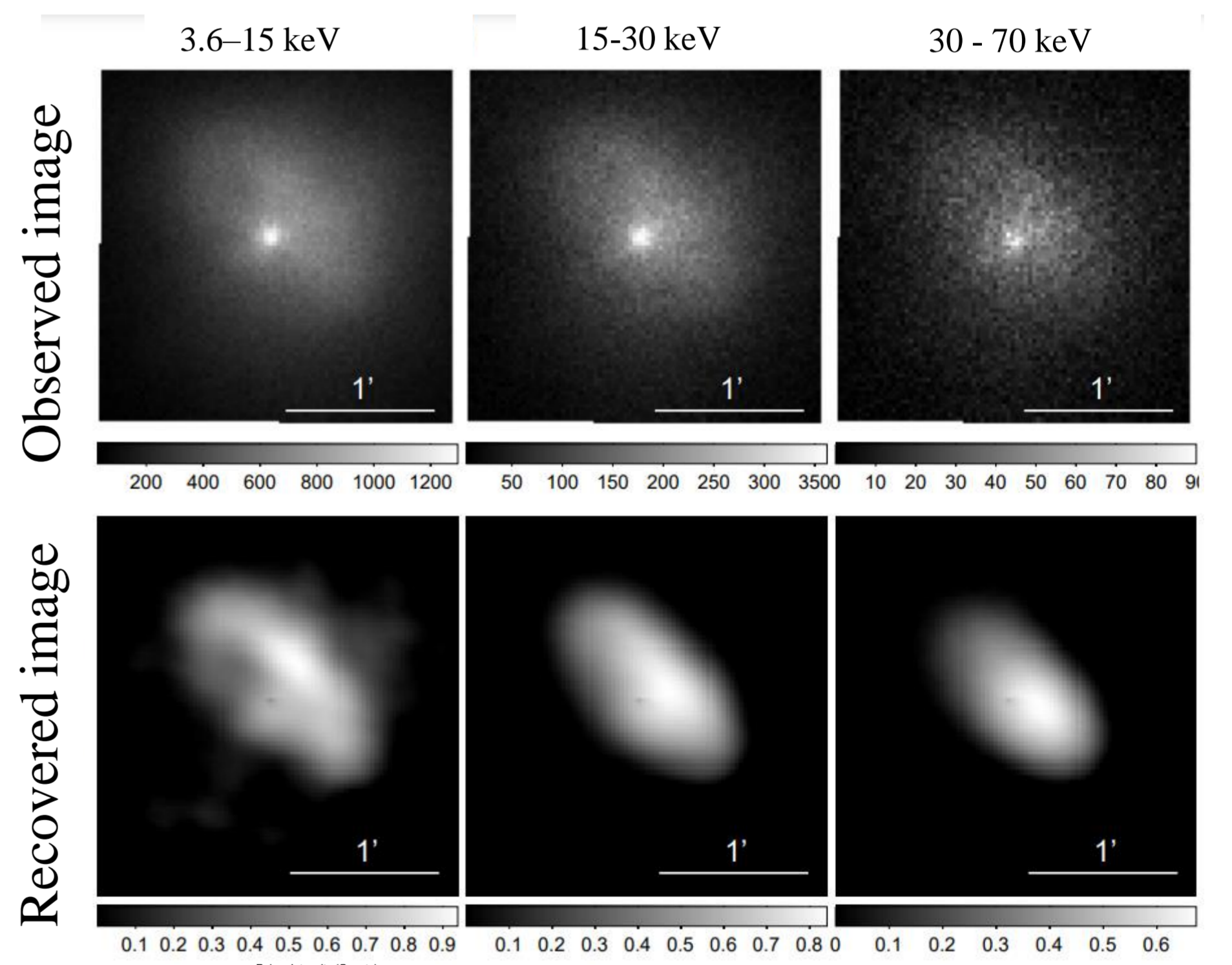
Z_f is a normalization factor. $\gamma > 0$ is a hyper-parameter.

Here, $f_{0,p}$ is the brightness of the pulsar in phase p . It is obtained by subtracting the total count of images in the pulse OFF phase from the total count of images in phase p .

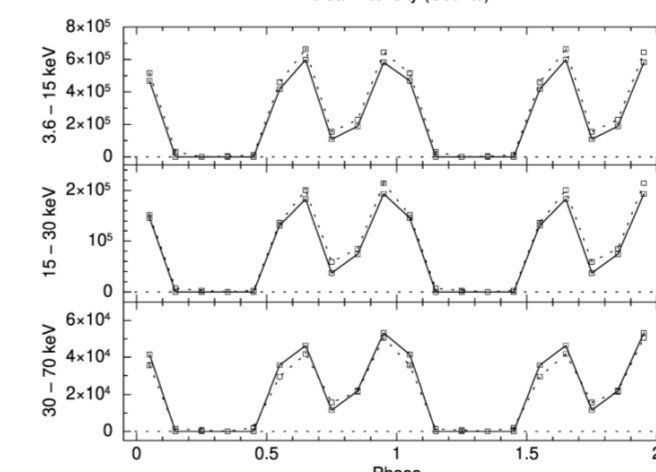
Since the pulsar may be glowing even in the pulse OFF phase, $f_{0,p}$ may be smaller than it actually is. To suppress the effect of this discrepancy, a hyperparameter (γ) was introduced.

We perform Maximum a posteriori probability estimation (MAP estimation) using EM algorithm. Hyper-parameters are determined by cross-validation.

Result



Pulse profile is also recovered.

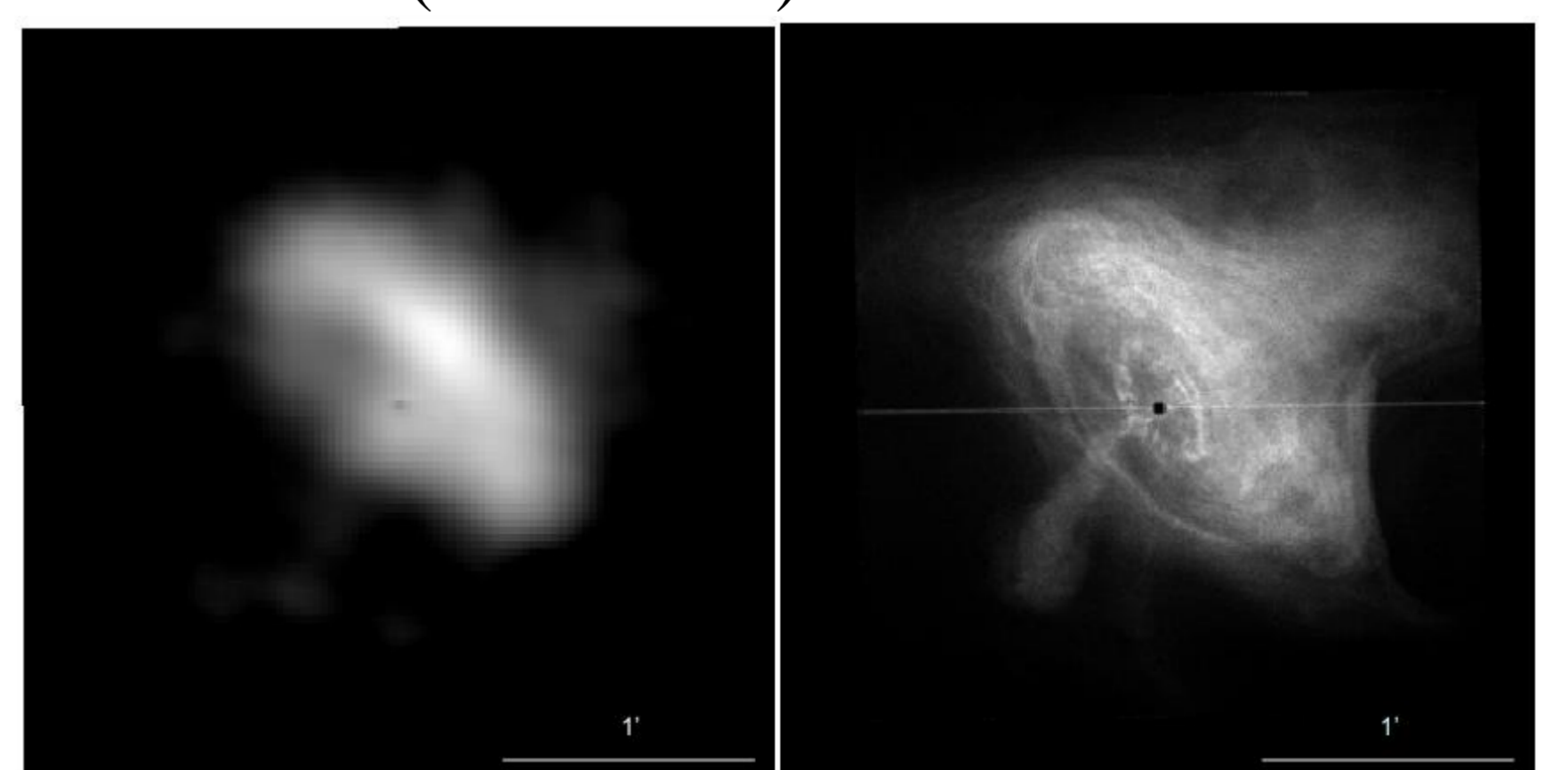


Dashed line: pulse profile given for pulse profile regularization

Solid line: Recovered pulse profile

Hitomi/HXT (3.6 - 15keV)

Chandra



Torus and jet structures can be seen in Hitomi/HXT!

Reference: M. Morii et al. (2024) PASJ,76,272